Tailoring Dispersion for Broadband Low-loss Optical Metamaterials Using Deep-subwavelength Inclusions

Zhi Hao Jiang[†], *Seokho Yun*[†], *Lan Lin, Jeremy A. Bossard, Douglas H. Werner,**and *Theresa S. Mayer**

Department of Electrical Engineering and Center for Nanoscale Science
The Pennsylvania State University
University Park, PA 16802, USA
E-mail: dhw@psu.edu and tsm2@psu.edu

Supplementary Information

Simulation comparison of metamaterial without deep-subwavelength nano-notches. To understand the role of the nano-notches in tailoring both the permittivity and permeability, the optimized metamaterial structure defined in Figure 2a was re-simulated without the subwavelength notches (*i.e.*, g = 0 nm). The scattering parameter amplitudes and effective medium parameters of the notch-free structure plotted in Figure S1a-d (bottom half of each plot) lend insight into the differences in device performance as well as the underlying physics. As can be seen in the permeability profiles (Figure S1c), the main magnetic resonance at 3.7 µm is broadened and almost saturated with the notches removed, exhibiting significant loss that is unfavorable in any transmissive application. The second magnetic resonance is shifted from 2.85 µm to 2.6 µm with a small quality factor increase. This shift can be attributed to the parallel momentum change in the (i,j)=(*1*,*0*) gap-SPP mode that arises when the notches are removed. This also gives rise to a higher cut-off frequency of the air hole waveguide array, thus producing a shorter effective plasma wavelength and sharper slope in the effective permittivity profile. The imbalanced permittivity and permeability result in a refractive index with an evanescent mode in the wavelength range of interest, as the imaginary part of the index becomes dominant. Another adverse consequence of this

imbalance is a poor impedance match, leading to near-unity reflection. Hence, the structure behaves more like a mirror within the targeted pass-band range.

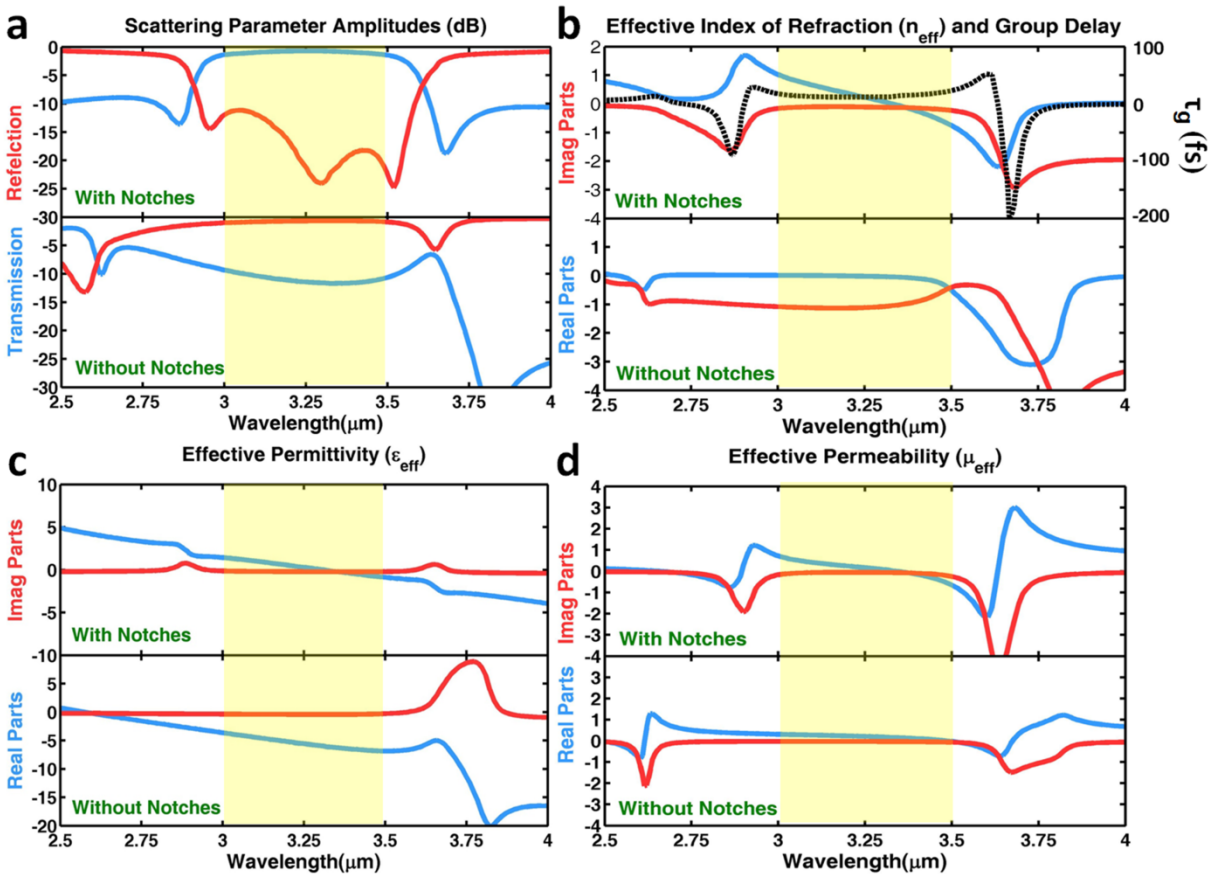

Figure S1. Simulation comparison for metamaterial with and without subwavelength nano-notches. Scattering parameters and effective properties for the metamaterial structure defined in Figure 2a (top) and of the same structure with the notches removed (bottom). (a) Transmission and reflection amplitudes showing poor stop band performance at the shorter wavelength range. (b) Effective index and group delay. (c) Effective permittivity. (d) Effective permeability.

Comparison with metamaterial filter optimized using unmodified fishnet structure.

To further demonstrate the importance of the deep-subwavelength nano-notches in tailoring the dispersive profiles of the effective medium parameters, we optimized a conventional fishnet structure without the notches. For this optimization, the constitutive materials and the cost function were kept the same as for the notched example presented in the main text in order to make a fair comparison with the modified fishnet design. The unit cell of the

optimized structure and its dimensions are depicted in Figure S2a, and the scattering parameter amplitudes are shown in Figure S2b along with those of the original structure introduced in Figure 2a. In the optimized fishnet without notches a pass-band can still be identified from 2.8 µm to 3.7 µm. However, within the pass-band the transmission intensity varies between 91.2% (-0.4 dB) and 47.9% (-3.2 dB), which is significantly lower than the average transmitted power of 82% (-0.9 dB) with a variation of only 9% (0.4 dB) achieved when adding the notches. In addition, the out-of-band rejection is poor, as the transmission remains above 10% (-10 dB) and reaches 21.4% (-6.7 dB) in both the short and long wavelength stop-band regions. The group delay of the optimized modified fishnet with the notches and the conventional fishnet without the notches are shown together in Fig. S2(c). The group delay of the conventional fishnet has a peak in the pass-band (2.8 ~ 3.7 µm) with a variation of 35 fs, which is about three times larger than that of the optmized modified fishnet. This comparison demonstrates the necessity of loading the fishnet structure with deep-subwavelength nano-notches to enable fine control of the effective medium parameters, which in turn facilitates the realization of the high-performance metamaterial filter.

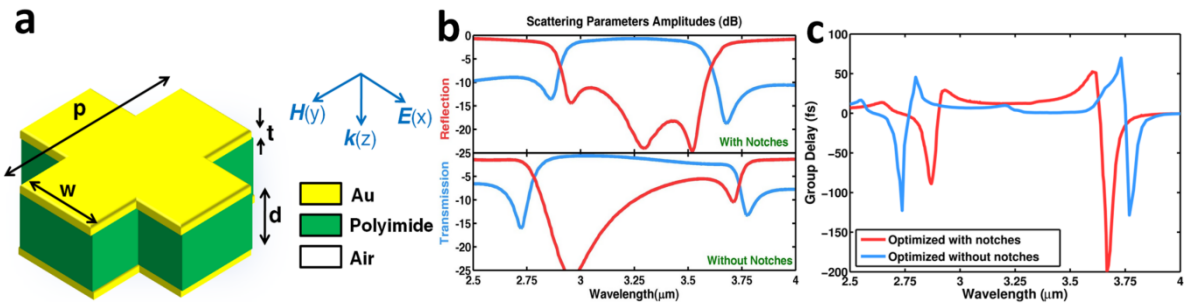

Figure S2. Optimized metamaterial design without notches and comparison of scattering parameters. (a) Conventional fishnet geometry optimized by a GA to have dimensions p=2390 nm, w=896 nm, t=30 nm and d=497 nm. (b) Transmission and reflection amplitudes of the optimized metamaterial filters with (top) and without the subwavelength nano-notches (bottom) showing that the notches are critical to enabling control of the primary and secondary magnetic resonances in the metamaterial response. (c) The group delay of the optimized nanostructure with (red) and without (blue) the subwavelength nano-notches.

Metamaterial filter simulation using dimensions measured from the fabricated sample. Additional numerical simulations were conducted for the modified nano-notched fishnet structure using the dimensions measured from the fabricated sample. Specifically, the fabricated structure has a sidewall angle of 89°, and a nano-notch sidewall length of g = 195 nm and 175 nm on the top and bottom surfaces, respectively. Figure S3a and S3b compare the measured transmission and reflection amplitudes with the simulated values using the ideal designed structure dimensions (Figure S3a) and the actual fabricated structure dimensions (Figure S3b). The results for the simulation using the fabricated dimensions show a stronger agreement with measurement in both the resonance positions and the bandwidth of the pass-band. This confirms that the slight discrepancies in the simulated properties of the ideal optimized structure and the measured properties of the fabricated structure are largely due to the small differences in feature sizes. Figure S3c compares the group delay of the metamaterial filter with the original design dimensions and the fabricated sample dimensions. Simulations of the fabricated structure show a slight band broadening in the group delay, similar to that observed in the transmission and reflection amplitudes. In the pass-band, the group delay profile remains relatively flat and has a variation of 15 fs. This group delay variation is only 3 fs larger than that of the ideal designed nanostructure.

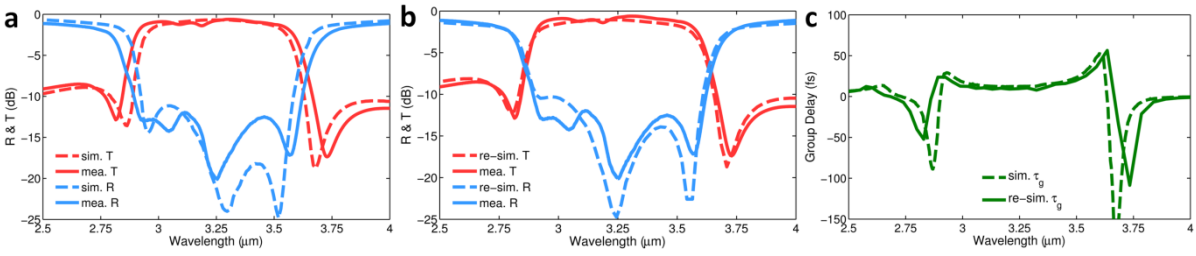

Figure S3. Additional scattering parameter amplitudes and group delay comparison of the modified fishnet nanostructure. (a) Simulated and measured transmission and reflection magnitudes (also shown in Fig. 3a). (b) Resimulated transmission and reflection magnitudes using the dimensions measured from the fabricated sample. The comparison between experiment and theory shows a stronger agreement. (c) Comparison of the simulated group delay of the optimized modified fishnet structure with the resimulated group delay using measured dimensions from the fabricated sample.

Extending the approach to broadband designs in the near-infrared. To show that this design approach can also be applied at shorter wavelengths in the near-infrared (near-IR), a metamaterial filter was optimized for the wavelength range around 1.55 μm following the same procedure. As shown in Figure S4a, the same nano-notched fishnet geometry was employed, and the metal was switched from gold (Au) to silver (Ag), which has smaller loss in the near-IR. All of the nanostructure dimensions were reduced relative to the mid-IR design shown in Figure 2a: unit cell size, p = 924 nm; thickness, d = 228 nm; nano-notch size, g = 62 nm. Specifically, g is ~1/3 the size of the original mid-IR design, and d is ~1/2 that of the original design. The smallest 62 nm feature size is easily patterned using the same lithographic process. In addition, the optimized etch should produce a sidewall angle of 89°, which would result in a bottom sidewall length of 54 nm and an averaged notch size of 58 nm, a variation of less than 6.5%. Based on the mid-IR example presented in the main text, which exhibits a variation in the average nano-notch size of 7.5%, it is expected that a fabricated near-IR metamaterial filter would maintain its high performance.

Figure S4b shows the optical properties of this near-IR modified fishnet nanostructure simulated using the HFSS full-wave solver. Within the 1 dB pass-band ranging from 1.40 μm to 1.65 μm, the average transmitted power at normal incidence is 77% (-1.2 dB), while the average reflected and absorbed intensities are 3% and 20%, respectively. The maximum variation in transmitted power is less than 11% (0.5 dB) across the full pass-band window. Even at this short wavelength range, a broad and flat transmission band can be achieved with a high transmission. Outside the pass-band, the impedance mismatch to free-space results in a high reflectivity, which reduces the average transmitted power to less than 10% (-10 dB). Here, the average reflected power is 68%, while the average absorbed power is 22%. Similar to the mid-IR design, within the band from 1.40 to 1.65 μm, the group delay fluctuates between 10 fs to 20 fs, indicating a small variation of only 10 fs. This near-IR design has slightly lower average in-band transmission compared to the optimized mid-IR structure.

However, this transmission is still high in comparison to previously demonstrated optical metamaterials and plasmonic nanostructures[2,36,41,45,46,47,48]. This confirms that deep-subwavelength inclusions can be used to tailor the dispersive properties of metamaterials at much shorter wavelengths, while also maintaining high optical performance. Due to the saturation of the magnetic resonances in metallodielectric structures in the visible range, we anticipate that nanoscale dielectric inclusions based on Mie scattering could provide controllable electric and magnetic resonant responses with low loss.

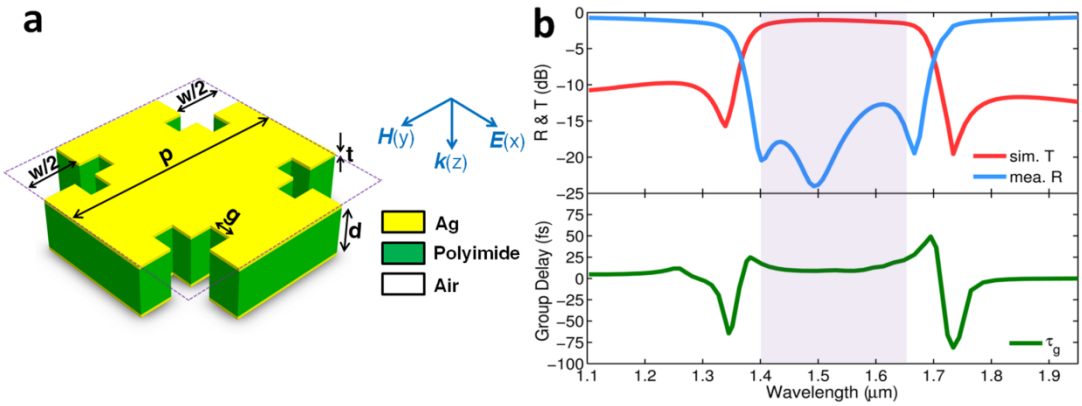

Figure S4. Broadband optical metamaterial band pass filter design for the near-IR wavelength range. (a) The geometry and dimensions of a single unit cell of the modified fishnet nanostructure. The optimized geometry dimensions are p=924 nm, w=493 nm, g=62 nm, t=34 nm and d=228 nm. (b) (top) Simulated transmission and reflection magnitudes for normally incident radiation showing broadband transmission over the highlighted region from 1.40 μm to 1.65 μm. (bottom) Simulated group delay τ_g shows minimal variation over the transmission window.